# Annealing effect on magnetic anisotropy in ultrathin (Ga,Mn)As*

Li Yan-Yong(李炎勇), Wang Hua-Feng(汪华锋), Cao Yu-Fei(曹玉飞), and Wang Kai-You(王开友)†

*The State Key Laboratory of Superlattices and Microstructure, Institute of Semiconductors, Chinese Academy of Sciences, Beijing* 100083, *China*

(Received 18 September 2012; revised manuscript received 17 October 2012)

We investigated the effect of low temperature annealing on magnetic anisotropy in 7-nm ultrathin $Ga_{0.94}Mn_{0.06}As$ devices by measuring the angle-dependent planar Hall resistance (PHR). Obvious hysteresis loops were observed during the magnetization reversal through the clockwise and counterclockwise rotations under low magnetic fields (below 1000 Gs, 1 Gs = $10^{-4}$ T), which can be explained by competition between Zeeman energy and magnetic anisotropic energy. It is found that the uniaxial anisotropy is dominant in the whole measured ferromagnetic range for both the as-grown ultrathin $Ga_{0.94}Mn_{0.06}As$ and the annealed one. The cubic anisotropy changes more than the uniaxial anisotropy in the measured temperature ranges after annealing. This gives a useful way to tune the magnetic anisotropy of ultrathin (Ga,Mn)As devices.

**Keywords:** magnetic anisotropy, planar Hall resistance, ultrathin (Ga,Mn)As

**PACS:** 75.50.Pp, 75.30.Gw, 75.30.Hx, 75.47.–m **DOI:** 10.1088/1674-1056/22/2/027504

## 1. Introduction

Ferromagnetic semiconductor (Ga,Mn)As has attracted great attention for both fundamental physics and potential applications since its discovery in the 1990s.[1–4] Most of the attractive properties of (Ga,Mn)As arise from magnetic anisotropy, holding great promise for the development of magnetic memory devices.[5,6] Magnetic moments prefer to follow magnetic easy axes in ferromagnetic materials due to magnetic anisotropic energy. In (Ga,Mn)As films, the magnetic anisotropy is complex due to the coexistence of the cubic anisotropy and uniaxial anisotropy,[7,8] while the latter dominates in most ferromagnetic metals. Magnetic anisotropy in (Ga,Mn)As films with thickness above 10 nm transforms from a biaxial mode at low temperatures to a uniaxial mode with increasing temperature, which has been attributed to the interplay between the natural cubic anisotropy of the zinc-blende structure and a uniaxial anisotropy that results from surface reconstruction.[9,10] However, it is found that the two-fold uniaxial anisotropy is dominant in the whole ferromagnetism temperature range for very thin (Ga,Mn)As films.[11] It is known that a magnetic anisotropic field can be tuned by strain, carrier density, and temperature. Each substitutional $Mn_{Ga}$ ion contributes one hole while the interstitial $Mn_I$ is a double donor which compensates holes in the system. Low temperature post growth annealing can increase the hole density through the out-diffusion of interstitial $Mn_I$ ions to the free surface.[12–14] Therefore, it is important to investigate the influence of low temperature annealing on the magnetic anisotropy in (Ga,Mn)As films.

In this paper, the method of measuring planar Hall resistance (PHR) with varying magnetic field direction at fixed magnitude has been used to investigate the magnetic anisotropy for both the as-grown and annealed 7-nm ultrathin $Ga_{0.94}Mn_{0.06}As$ devices. Because the PHR is very sensitive to the magnitude and orientation of the local magnetization, this method can provide a panorama of magnetization reversal for continuously varying direction of external magnetic field, which can give information on the formation of the domain structure during the magnetization reversal. So angle-dependent PHR is a powerful technique to detect the magnetic anisotropy and magnetic domain structures in (Ga,Mn)As.[15] Here we also report our quantitative investigation of the temperature dependence of magnetic anisotropic coefficients in 7-nm ultrathin $Ga_{0.94}Mn_{0.06}As$ devices before and after 180 °C low temperature annealing, by measuring Hall configuration.

## 2. Experiments

The $Ga_{0.94}Mn_{0.06}As$ film was grown on semi-insulating GaAs (001) substrate by molecular beam epitaxy (MBE) at around 240 °C. A 150-nm thick undoped GaAs buffer layer was grown first, followed by 7-nm $Ga_{0.94}Mn_{0.06}As$ epilayer. A circular device with a diameter of 16 μm, as shown in Fig. 1(a), for the ultrathin $Ga_{0.94}Mn_{0.06}As$ film was fabricated by standard electron beam lithography and wet etching. The metallic Ohmic bond pads along the major in-plane axes were deposited with 50-nm Ti and 150-nm Au by electron beam evaporation. For comparison, a device with the same structure with a 25-nm $Ga_{0.94}Mn_{0.06}As$ epilayer was also fabricated. The as-grown devices were annealed at 180 °C for 48 hours in air to investigate the influence of low temperature annealing on magnetic anisotropy.

*Project supported by the National Basic Research Program of China (Grant No. 2011CB922200), the National Natural Science Foundation of China (Grant No. 11174272), and the Engineering and Physical Sciences Research Council–National Natural Science Foundation Joint (Grant No. 10911130232/A0402).

†Corresponding author. E-mail: kywang@semi.ac.cn

© 2013 Chinese Physical Society and IOP Publishing Ltd 

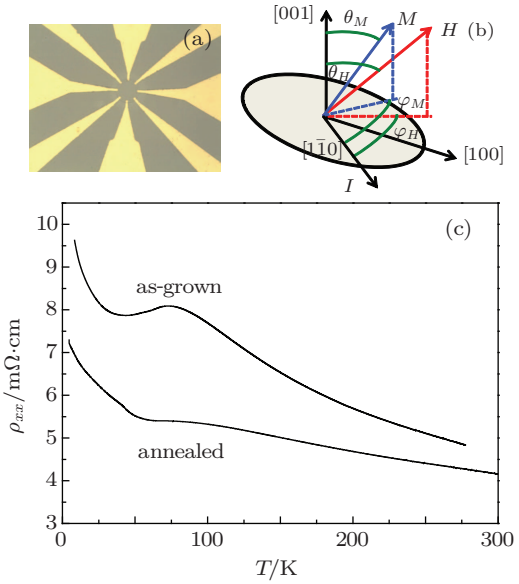



**Fig. 1.** (color online) (a) Photograph of the $Ga_{0.94}Mn_{0.06}As$ device with eight Ti/Au contacts. Diameter of the circle is 16 μm. (b) Sketch of the definition of the external magnetic field, magnetization orientation, and the major crystalline axes. (c) Temperature dependence of the resistivity for both the as-grown and annealed 7-nm ultrathin $Ga_{0.94}Mn_{0.06}As$ devices.

Temperature dependence of the sheet resistance (R-T) for both the as-grown & annealed 7-nm ultrathin $Ga_{0.94}Mn_{0.06}As$ devices with current along the [1$\bar{1}$0] orientation was measured by using the standard four probes method and plotted in Fig. 1(c). Angle-dependent PHR was measured under a series of external magnetic fields at 3.5 K for counterclockwise rotation (CCW) and clockwise rotation (CW), respectively, with the current applied along the orientation. Before each rotation, 5000 Gs was applied to initialize the magnetization. The measured experimental results for both the as-grown and annealed 7-nm $Ga_{0.94}Mn_{0.06}As$ samples are shown in Fig. 2. In addition, PHR for both the as-grown and annealed $Ga_{0.94}Mn_{0.06}As$ devices at a series of temperatures was measured to investigate the temperature dependence of the magnetic anisotropy.

## 3. Results and discussion

The singularity in the temperature derivative of the resistivity $d\rho/dT$ can be used to determine the Curie temperature ($T_C$).[16] $T_C$ is found to be (64±2) K, and it increases to (69±2) K after low temperature annealing for the 7-nm ultrathin $Ga_{0.94}Mn_{0.06}As$ device. The resistivity of the device is decreased by about 49%, indicating an increment of the hole density. However, it is found that $T_C$ for 25-nm reference device increases from (57±2) K to (112±2) K after low temperature annealing. The low temperature annealing removes the interstitial $Mn_I$ ions through out-diffusion,[13,17] resulting in the increment of Curie temperature and reduction of resistivity. Our experimental results suggest that a higher percentage of Mn ions occupy the interstitial sites with increasing thickness of the films. In order to quantitatively obtain the change of the hole density caused by low temperature annealing, Hall measurements at rather low temperature and high magnetic field have been performed because of the strong anomalous Hall effect, where the magnetization is constant – i.e. fully saturated (because the magnetization is easily saturated at low temperatures). The Hall resistance $R_{xy}$ for ferromagnetic materials is empirically known to be a sum of an ordinary Hall term and an anomalous Hall term as:[18]

$$R_{xy} = R_0 B/d + R_A M/d, \tag{1}$$

where $R_0$ is the ordinary Hall coefficient, $R_A$ the anomalous Hall coefficient, $d$ the sample thickness, and $M$ the magnetization of the magnetic materials; $R_A$ is proportional to longitudinal resistance $R_{xx}^{\gamma}$, with regard to which it has been suggested that the side-jump is likely to be the dominant mechanism in (Ga,Mn)As.[19] An alternative treatment of the anomalous Hall effect also gives $\gamma = 2$,[20] in which it is considered to arise directly from the band structure of the ferromagnet. According to the high field Hall measurements using Eq. (1), we have obtained the hole density $3.4\times10^{20}$ cm$^{-3}$ and $4.5\times10^{20}$ cm$^{-3}$ for the as-grown and annealed ultrathin 7-nm $Ga_{0.94}Mn_{0.06}As$ device, respectively. The increment of hole density of about 30% after low temperature annealing is in good agreement with the theoretical prediction and previous experimental findings, through the relationship between the change of $T_C$ and hole density.[21,22]

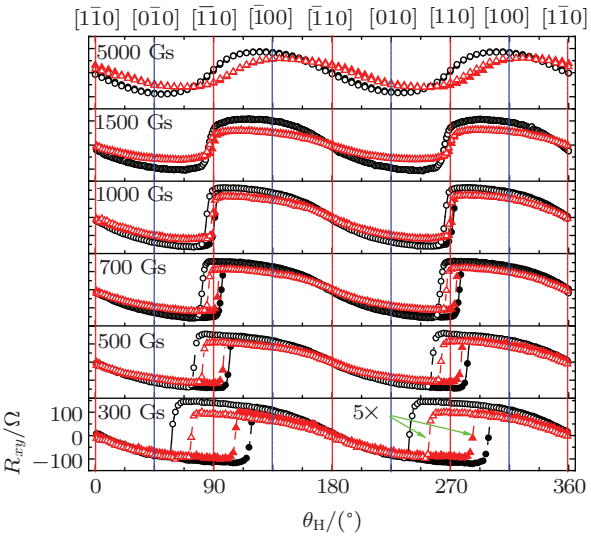



**Fig. 2.** (color online) Angle-dependent planar Hall resistance for as-grown (circular black symbols) and annealed (triangular red symbols) 7-nm $Ga_{0.94}Mn_{0.06}As$ devices measured under different external magnetic fields at 3.5 K, where the magnitude of PHR for the annealed device has been multiplied by a factor of 5. The hollow symbols represent clockwise rotations and the solid ones represent counterclockwise rotations, respectively.

Planar Hall resistance arises as a result of the nonequivalent components of the resistivity tensor perpendicular and parallel to the magnetization direction, leading to the appearance of the off-diagonal resistivity components. According to

the definition of PHR, the electric field in a ferromagnetic device is given by:[23]

$$E_x = j\rho_\perp + j(\rho_\parallel - \rho_\perp)\cos^2\varphi_M,$$
$$E_y = j(\rho_\parallel - \rho_\perp)\sin\varphi_M\cos\varphi_M, \quad (2)$$

in which $j$ is the current density, $\rho_\parallel$ and $\rho_\perp$ are the longitudinal resistivity for current parallel and perpendicular to the magnetization, and $\varphi_M$ is the angle between the magnetization orientation and current direction. The upper formula in function (2) represents the AMR and the lower one is for the PHR. From function (2), we find that the PHR is directly related to the local magnetic states in the device.

In Fig. 2, readily apparent hysteresis loops along $\langle 110\rangle$ directions are observed in the CW and CCW PHR curves in the as-grown and annealed 7-nm ultrathin $Ga_{0.94}Mn_{0.06}As$ devices with external magnetic fields below 1000 Gs. The hysteresis loops become wider with decreasing external magnetic fields, implying the appearance of a multidomain structure. Upon further increasing the external magnetic fields, the PHR curves of $Ga_{0.94}Mn_{0.06}As$ gradually transform into sinusoidal curves without hysteresis loops, indicative of a coherent rotation. The experimental CW and CCW PHR curves for the annealed 7-nm $Ga_{0.94}Mn_{0.06}As$ device have been multiplied by a factor of 5, which is also shown in Fig. 2. The magnitude of the PHR is strongly suppressed after low temperature annealing, which is due to the decrease of the resistivity of the device after low temperature annealing. The hysteresis transition ranges become smaller after low temperature annealing. Unlike the 7-nm ultrathin $Ga_{0.94}Mn_{0.06}As$ devices, readily apparent hysteresis loops are observed along both $\langle 110\rangle$ and $\langle 1\bar{1}0\rangle$ orientations between CW and CCW PHR curves for 25-nm reference $Ga_{0.94}Mn_{0.06}As$ devices, which is similar to previously reported findings.[24–26] This four-fold symmetry originates from the cubic magnetic anisotropy dominating the magnetic free energy.

The detailed characteristics of the PHR curves during the magnetization reversal result from the competition between the magnetic anisotropy energy and Zeeman energy in the in-plane magnetized devices, which can be explained by the function of magnetic free energy,[27]

$$\begin{aligned} F \;=\; & -MH[\cos\theta_M\cos\theta_H + \sin\theta_M\sin\theta_H\cos(\varphi_M-\varphi_H)] \\ & + 2\pi M^2\cos^2\theta_M + \frac{1}{2}M[-H_{U\perp}\cos^2\theta_M \\ & - H_{U\parallel}\sin^2\theta_M\sin^2\varphi_M \\ & - \frac{1}{2}H_{C\perp}\cos^4\theta_M - \frac{1}{4}H_{C\parallel}\sin^4\theta_M\cos^2 2\varphi_M], \end{aligned} \quad (3)$$

in which the first term describes the Zeeman energy, the second term represents the shape anisotropy energy, and the last term gives magnetic anisotropy energy; $H_{U\parallel}$ and $H_{C\parallel}$ are in-plane uniaxial and cubic anisotropic fields, $H_{U\perp}$ and $H_{C\perp}$ are perpendicular uniaxial and cubic anisotropic fields, $H$ is the external magnetic field, and $\varphi_H$ indicate the angles of magnetization and external magnetic field to direction; $\theta_M$ and $\theta_H$ represent the out-plane components of the magnetization and external magnetic field. With in-plane magnetic easy axes and the external magnetic field, $\theta_M$ and $\theta_H$ are both 90° in our experimental configuration. Function (3) can be transformed into,

$$\begin{aligned} F \;=\; & -MH\cos(\varphi_M-\varphi_H) \\ & - \frac{MH_{C\parallel}}{8}\cos^2 2\varphi_M - \frac{MH_{U\parallel}}{2}\cos^2\varphi_M. \end{aligned} \quad (4)$$

Under high magnetic fields, the Zeeman term dominates the magnetic free energy. Therefore, the direction of magnetization follows the external magnetic field closely. As the external magnetic field is decreased gradually, magnetic anisotropy energy plays a more important role in controlling the magnetization reversal. Thus the number of local magnetic free energy minima will be increased. The magnetization of the device will prefer to maintain the local energy minimum states. Specifically, in the PHR transition hysteresis ranges, magnetization moments need to overcome the pinning fields to enter the lower neighboring energy minima.[26] In this process, the transition happens only in the areas where pinning fields are smaller than $\Delta F/M$, in which $\Delta F$ is the difference between two neighboring energy minima. That is the reason hysteresis loops appear in the PHR curves.

The cubic magnetic anisotropy easy axes and uniaxial magnetic easy axes in $Ga_{0.94}Mn_{0.06}As$ are along the $\langle 100\rangle$ and $\langle 1\bar{1}0\rangle$ orientations, respectively. Therefore, when the uniaxial anisotropy dominates the magnetic free energy, the hysteresis loops appear when the magnetization crosses the uniaxial hard axes $\langle 110\rangle$. During rotation of the external magnetic fields crossing $\langle 110\rangle$ directions, fractional domains populate one easy axis and the remaining domains populate the neighboring easy axis, forming multidomain states. So the behavior of magnetization is not coherent rotation in these transition ranges but nucleation and expansion of domains.[15] In the 25-nm reference $Ga_{0.94}Mn_{0.06}As$ device, the cubic magnetic anisotropy dominates at this temperature, the orientations of neighboring energy minima follow four $\langle 100\rangle$ directions and the difference of the neighboring easy axes will be approximated at 90°. Therefore, hysteresis loops in the PHR curves can appear in both $\langle 110\rangle$ and $\langle 1\bar{1}0\rangle$ directions at low external magnetic fields as reported.

In order to obtain the cubic anisotropic field $H_{C\parallel}$ and uniaxial anisotropic field $H_{U\parallel}$ in the as-grown and annealed ultrathin $Ga_{0.94}Mn_{0.06}As$ devices quantitatively, we fit the relationship between and $\varphi_H$ through the experimental PHR values on the condition of minimal magnetic free energy. According to the functions (2) and (4), where $\partial F/\partial\varphi_M = 0$, we have ob-

tained

$$\varphi_H = \varphi_M + \arcsin\left[\frac{1}{H}\left(\frac{H_{C\parallel}}{4}\sin 4\varphi_M + \frac{H_{U\parallel}}{2}\sin 2\varphi_M\right)\right]. \quad (5)$$

The relationship between $\varphi_H$ and for the 7-nm as-grown ultrathin $Ga_{0.94}Mn_{0.06}As$ device under 1500 Gs at 3.5 K is shown in Fig. 3. Under this external magnetic field strength, the external magnetic field is slightly larger than the anisotropic field and the hysteresis loops almost disappear. Therefore, both the cubic anisotropy $H_{C\parallel}$ and uniaxial anisotropy $H_{U\parallel}$ can be obtained easily by fitting the curve with the function (5). $H_{C\parallel} = (446 \pm 41)$ Gs and $H_{U\parallel} = (1040 \pm 20)$ Gs have been obtained in Fig. 3.

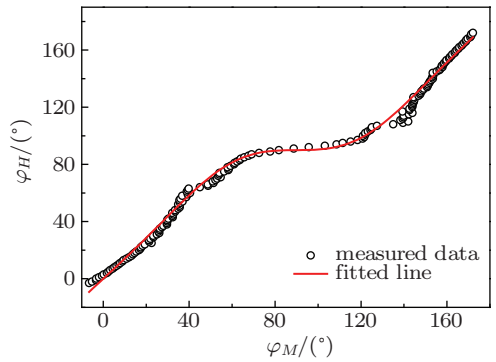



**Fig. 3.** (color online) The angular relationship between the magnetization and external magnetic field for as-grown ultrathin $Ga_{0.94}Mn_{0.06}As$ film under 1500 Gs at 3.5 K.

We also performed the same method to obtain the temperature dependence of $H_{C\parallel}$ and $H_{U\parallel}$ for both the as-grown and annealed devices, as shown in Fig. 4.

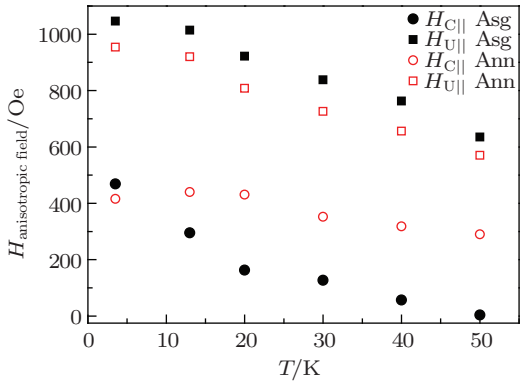



**Fig. 4.** (color online) Temperature dependence of magnetic anisotropic fields obtained from fitting the experimental data using function (4) for as-grown (solid symbols) and annealed (open symbols) 7-nm ultrathin $Ga_{0.94}Mn_{0.06}As$ devices, 1 Oe = 79.5775 A/m.

The uniaxial magnetic anisotropy fields are larger than the cubic magnetic anisotropy fields in the whole ferromagnetic temperature range for both the as-grown and annealed 7-nm ultrathin $Ga_{0.94}Mn_{0.06}As$ devices, indicating the dominance of the uniaxial anisotropy. After low temperature annealing, the uniaxial magnetic anisotropic fields decrease by less than 15% in the whole temperature range. However, except at very low temperatures, the cubic magnetic anisotropic fields after low temperature annealing are much larger than in the as-grown sample and the relative changes of the cubic magnetic anisotropic fields increase with rising temperature. The strong modulation of the magnetic anisotropy after low temperature annealing is attributed to the increment of the hole density, as low temperature annealing can increase the effective Mn density and total magnetization. Therefore varying the carrier density in $Ga_{0.94}Mn_{0.06}As$ is a good way to tune the magnetic anisotropy. For example, electric gating can effectively tune the carrier density in very thin ferromagnetic devices, which can be used to modify the magnetic anisotropy. This has already been demonstrated by many groups.[28–30]

## 4. Summary

In conclusion, we have carefully investigated the effect of low temperature annealing on the magnetic anisotropy of 7-nm ultrathin $Ga_{0.94}Mn_{0.06}As$ devices by measuring angle-dependent planar Hall resistance. The magnitude of PHR after low temperature annealing becomes 20% of that in the as-grown device. We find that the uniaxial anisotropy is dominant in the whole ferromagnetic temperature range for both the as-grown and annealed $Ga_{0.94}Mn_{0.06}As$ devices. In addition, the relative changes of the cubic anisotropy increase with rising temperature, while the uniaxial anisotropy is slightly reduced in the process. The changes of magnetic anisotropy after low temperature annealing are attributed to the increment of the hole density. Therefore, the magnetic anisotropy in ultrathin ferromagnetic (Ga,Mn)As devices can be largely modified by tuning carrier density.

## Acknowledgement

Wang Kai-You acknowledges support of the Chinese Academy of Sciences' "100 Talent Program."

## References

[1] Ohno H, Shen A, Matsukura F, Oiwa A, Endo A, Katsumoto S and Iye Y 1996 *Appl. Phys. Lett.* **69** 363
[2] Matsukura F, Sawicki M, Dietl T, Chiba D and Ohno H 2004 *Physica E: Low-dimensional Systems and Nanostructures* **21** 1032
[3] Chiba D, Sawicki M, Nishitani Y, Nakatani Y, Matsukura F and Ohno H 2008 *Nature* **455** 515
[4] Chen L, Yang X, Yang F, Zhao J, Misuraca J, Xiong P and von Molnaár S 2011 *Nano Lett.* **11** 2584
[5] Myers E B, Ralph D C, Katine J A, Louie R N and Buhrman R A 1999 *Science* **285** 867
[6] Lee S, Yoo T, Lee H, Khym S, Liu X and K. Furdyna J 2011 *Jpn. J. Appl. Phys.* **50** 04DM02
[7] Kim J, Shin D Y, Lee S, Liu X and Furdyna J K 2008 *Phys. Rev.* B **78** 075309
[8] Kim J, Shin D Y, Yoo T, Kim H, Lee S, Liu X and Furdyna J K 2008 *J. Appl. Phys.* **103** 07D101
[9] Welp U, Vlasko-Vlasov V K, Liu X, Furdyna J K and Wojtowicz T 2003 *Phys. Rev. Lett.* **90** 167206

[10] Wang K Y, Sawicki M, Edmonds K W, Campion R P, Maat S, Foxon C T, Gallagher B L and Dietl T 2005 *Phys. Rev. Lett.* **95** 217204

[11] Rushforth A W, Výborný K, King C S, Edmonds K W, Campion R P, Foxon C T, Wunderlich J, Irvine A C, Vašek P, Novák V, Olejník K, Sinova J, Jungwirth T and Gallagher B L 2007 *Phys. Rev. Lett.* **99** 147207

[12] Stanciu V, Wilhelmsson O, Bexell U, Adell M, Sadowski J, Kanski J, Warnicke P and Svedlindh P 2005 *Phys. Rev.* B **72** 125324

[13] Edmonds KW, Bogusławski P, Wang K Y, Campion R P, Novikov S N, Farley N R S, Gallagher B L, Foxon C T, Sawicki M, Dietl T, Buongiorno Nardelli M and Bernholc J 2004 *Phys. Rev. Lett.* **92** 037201

[14] Deng J J, Zhao J H, Jiang C P, Zhang Y, Niu Z C, Yang F H, Wu X G and Zheng H Z 2005 *Chin. Phys. Lett.* **22** 466

[15] Kim J, Lee H, Yoo T, Lee S, Liu X and Furdyna J K 2011 *Phys. Rev.* B **84** 184407

[16] Novák V, Olejník K, Wunderlich J, Cukr M, Výborný K, Rushforth A W, Edmonds K W, Campion R P, Gallagher B L, Sinova J and Jungwirth T 2008 *Phys. Rev. Lett.* **101** 077201

[17] Yu K M, Walukiewicz W, Wojtowicz T, Kuryliszyn I, Liu X, Sasaki Y and Furdyna J K 2002 *Phys. Rev.* B **65** 201303

[18] Chien C L and Westgate C R 1980 *The Hall Effect and Its Applications* (California: Plenum Press)

[19] Dietl T, Matsukura F, Ohno H, Cibert J and Ferrand D 2003 *Hall Effect and Magnetoresistance in P-Type Ferromagnetic Semiconductors*: *Recent Trends in Theory of Physical Phenomena in High Magnetic Fields* (Netherlands: Springer) p. 197

[20] Jungwirth T, Niu Q and MacDonald A H 2002 *Phys. Rev. Lett.* **88** 207208

[21] Wang K Y, Edmonds K W, Campion R P, Gallagher B L, Farley N R S, Foxon C T, Sawicki M, Boguslawski P and Dietl T 2004 *J. Appl. Phys.* **95** 6512

[22] Jungwirth T, Wang K Y, Mašek J, Edmonds K W, König J, Sinova J, Polini M, Goncharuk N A, MacDonald A H, Sawicki M, Rushforth A W, Campion R P, Zhao L X, Foxon C T and Gallagher B L 2005 *Phys. Rev.* B **72** 165204

[23] Tang H X, Kawakami R K, Awschalom D D and Roukes M L 2003 *Phys. Rev. Lett.* **90** 107201

[24] Kim J, Lee S, Lee S, Liu X and Furdyna J K 2010 *Solid State Commun.* **150** 27

[25] Limmer W, Daeubler J, Dreher L, Glunk M, Schoch W, Schwaiger S and Sauer R 2008 *Phys. Rev.* B **77** 205210

[26] Kim J, Yoo T, Chung S, Lee S, Liu X and Furdyna J K 2009 *J. Appl. Phys.* **105** 07C501

[27] Lee S, Chung J H, Liu X, Furdyna J K and Kirby B J 2009 *Materials Today* **12** 14

[28] Olejník K, Owen M H S, Novák V, Mašek J, Irvine A C, Wunderlich J and Jungwirth T 2008 *Phys. Rev.* B **78** 054403

[29] Owen M H S, Wunderlich J, Novák V, Olejník K, Zemen J, Vyborny K, Ogawa S, Irvine A C, Ferguson A J, Sirringhaus H and Jungwirth T 2009 *New J. Phys.* **11** 023008

[30] Endo M, Chiba D, Shimotani H, Matsukura F, Iwasa Y and Ohno H 2010 *Appl. Phys. Lett.* **96** 022515